Available online at www.sciencedirect.com
ScienceDirect
ELSEVIER
Computers & Fluids 35 (2006) 1459–1463
computers & fluids
www.elsevier.com/locate/compfluid

Technical Note

Low-dissipation and low-dispersion fourth-order Runge–Kutta algorithm

Julien Berland *, Christophe Bogey, Christophe Bailly

Laboratoire de Mécanique des Fluides et d'Acoustique, UMR CNRS 5509, Ecole Centrale de Lyon, 69134 Ecully, France

Received 7 January 2005; received in revised form 12 April 2005; accepted 14 April 2005
Available online 1 August 2005

Abstract

An optimized explicit low-storage fourth-order Runge–Kutta algorithm is proposed in the present work for time integration. Dispersion and dissipation of the scheme are minimized in the Fourier space over a large range of frequencies for linear operators while enforcing a wide stability range. The scheme remains of order four with nonlinear operators thanks to the low-storage algorithm. Linear and nonlinear propagation problems are finally solved to illustrate the accuracy of the present Runge–Kutta scheme.

1. Introduction

Past decade works on numerical methods aimed at designing low-dissipative, low-dispersive and large spectral bandwidth numerical algorithms. Spatial discretization schemes have first gained interests: Tam and Webb [1] gave for instance the explicit DRP schemes, Lele [2] developed compact finite differences, and recently Bogey and Bailly [3] built up explicit finite differences and selective filters accurate for waves down to four points per wavelength to perform direct computation of aerodynamic noise [4]. Time integration has then been optimized with the same aim in view, especially using Runge–Kutta (RK) algorithms [5].

In computational fluid dynamics applications, standard third- and fourth-order RK algorithms are commonly used because of their large stability range. Nevertheless, stability considerations are important but not sufficient when dealing with aeroacoustic purposes. Hu et al. [5] and Bogey and Bailly [3] developed RK algorithms optimized for linear operators, whose coefficients are determined to minimize dispersion and dissipation errors over a given range of frequencies. The advantages of the algorithms also include low-storage requirements since only two memory slots are needed per variable. However, the algorithms used cannot ensure an order of accuracy higher than two for nonlinear operators. To allow high order with nonlinear operators, Williamson [6] first proposed a low-storage algorithm. Stanescu and Habashi [7] developed more recently RK algorithms including a six-stage RK displaying the properties of one of the Hu's schemes [5] for linear operators while being of order four with nonlinear operators, but with weak stability properties.

In the present paper, a low-storage six-stage RK algorithm, optimized for linear operators, of fourth-order in nonlinear and with a wide stability range is proposed. The calculation of the algorithm coefficients is first described. Linear and nonlinear propagation test cases are then solved to illustrate the scheme accuracy. Finally, concluding remarks are drawn in the last section. Note that similar results are to be published by Calvo et al. [8]. The scheme proposed here is however built up using another linear optimization method and is in the continuity of the works of Bogey and Bailly

* Corresponding author. Fax: +33 4 72 18 91 43.
E-mail addresses: julien.berland@ec-lyon.fr (J. Berland), christophe.bogey@ec-lyon.fr (C. Bogey), christophe.bailly@ec-lyon.fr (C. Bailly).

0045-7930/$ - see front matter
doi:10.1016/j.compfluid.2005.04.003

[3] and Berland et al. [9]. The test cases are in addition different. They are especially more relevant to acoustic problems than those solved by Calvo et al. [8].

2. Low-storage fourth-order six-stage Runge–Kutta algorithm

Consider the time integration using Runge–Kutta (RK) algorithms of the following differential equation:

$$\frac{\partial u}{\partial t} = F(u,t)$$

where the operator F is a function of the unknown u and of time t. Several formulations of RK schemes have been built up to improve accuracy and to reduce storage requirements [3,5,7]. Hu et al. [5] proposed the following low-storage s-stage algorithm to compute the time integration from $u^n = u(n\Delta t)$ to $u^{n+1} = u[(n+1)\Delta t]$:

$$u^{n+1} = u^n + \sum_{j=1}^{s} \gamma_j \Delta t^j F^j(u) \tag{1}$$

where $F^j = \overbrace{F \circ \cdots \circ F}^{j}$, Δt is the time step and γ_j are the algorithm coefficients. However, order of accuracy of the algorithm cannot be greater than two when used with nonlinear operators. To increase order of accuracy in nonlinear, Williamson's [6] formulation, which only requires two storage locations per variable, is used:

$$\text{for } i = 1 \ldots s \begin{cases} \omega_i = \alpha_i \omega_{i-1} + \Delta t F(u_{i-1}, t_i) \\ u_i = u_{i-1} + \beta_i \omega_i \end{cases} \tag{2}$$

where s is the number of stage, Δt the time step, $u_0 = u^n$, $u^{n+1} = u_s$, $\omega_0 = 0$ and $t_i = (n + c_i)\Delta t$. α_i and β_i are the coefficients of the algorithm. For an explicit scheme, α_1 is set to zero.

In the present work, an explicit fourth-order six-stage RK scheme based on algorithm (2) and referred to as RK46-NL is designed. Its coefficients are computed using the method proposed by Stanescu and Habashi [7]: using algorithm (1), a RK scheme is built up by optimizing coefficients γ_j in the Fourier space for linear operators. The algorithm, referred to as RK46-L, is of order four in linear but of order two in nonlinear. Coefficients γ_j are then used as a starting point to determine coefficients α_i and β_i of the algorithm (2), which permits fourth-order accuracy whether the operator is linear or nonlinear.

First assume F is a linear operator which does not depend on the time variable t. Following Hu et al. [5], applying temporal Fourier transform to (1) gives the amplification factor of the algorithm:

$$G(\omega\Delta t) = \frac{\hat{u}^{n+1}(\omega\Delta t)}{\hat{u}^n(\omega\Delta t)} = 1 + \sum_{j=1}^{s} \gamma_j (i\omega\Delta t)^j$$

For comparison with the exact amplification factor $\exp(i\omega\Delta t)$, it is written as $|G(\omega\Delta t)|\exp(i\omega^*\Delta t)$. At each time step for an angular frequency ω, the amount of dissipation is $1 - |G(\omega\Delta t)|$ and the phase error is $\omega\Delta t - \omega^*\Delta t$.

Coefficients γ_j of the RK46-L algorithm are provided in Table 1. They are determined as follows: fourth-order accuracy is achieved by setting $\gamma_j = 1/j!$, for $j = 1$ to $j = 4$. In the same way as in Bogey and Bailly [3], the two remaining coefficients γ_5 and γ_6 are chosen by optimizing the dispersion and dissipation for $\pi/16 < \omega\Delta t < \pi/2$, for waves between 32 and 4 time steps per period with $T/\Delta t = 2\pi/\omega\Delta t$. Note that they are within 2% of the coefficients found by Calvo et al. [8].

Using the γ_j coefficients and adding order conditions [7] that ensure fourth-order accuracy for nonlinear operators give a system of equations leading to the coefficients α_i and β_i of the RK46-NL. Nevertheless, one parameter remains free and must be imposed. The value of $\beta_6 = 0.27$ is chosen from nonlinear test cases as shown in detail in [9]. The coefficients of the RK46-NL scheme are given in Table 1.

First stability is checked. The stability limits obtained for an amplification rate $|G(\omega\Delta t)| = 1$ are reported in Table 2 for the standard fourth-order four-stage RK scheme (RK44), the fourth-order six-stage RK developed by Stanescu and Habashi [7] (RK46-Stanescu), the second-order six-stage RK of Bogey and Bailly [3] (RK26-Bogey) and the present algorithm (RK46-NL). The stability limit of the RK44 algorithm is about 2 time steps per period. The RK26-Bogey and RK46-NL algorithms have a similar limit of $\omega\Delta t = 3.9$ corresponding to 1.6 time steps per period. The stability limit of the RK46-Stanescu algorithm is close to $\omega\Delta t = 1.7$, i.e. about 3.8 time steps per period. The limit of the

Table 1
Coefficients γ_i of the RK46-L algorithm and coefficients α_i and β_i and c_i of the RK46-NL scheme

i	γ_i	α_i	β_i	c_i
1	1	0.0	0.032918605146	0.0
2	1/2	−0.737101392796	0.823256998200	0.032918605146
3	1/6	−1.634740794341	0.381530948900	0.249351723343
4	1/24	−0.744739003780	0.200092213184	0.466911705055
5	0.007856772044	−1.469897351522	1.718581042715	0.582030414044
6	0.000959998595	−2.813971388035	0.27	0.847252983783

Table 2
Stability, dissipation and dispersion limits of the RK schemes in points per period $T/\Delta t = 2\pi/\omega\Delta t$

	Stability $\lvert G(\omega\Delta t)\rvert < 1$	Dissipation $1 - \lvert G(\omega\Delta t)\rvert < 5\times10^{-4}$	Dispersion $\lvert\omega^*\Delta t - \omega\Delta t\rvert/\pi < 5\times10^{-4}$
RK44	2.22	9.65	8.40
RK46-Stanescu	3.80	5.32	3.13
RK26-Bogey	1.59	3.29	5.03
RK46-NL	1.65	3.19	4.10

RK46-NL scheme is thus more than two times larger than this of the RK46-Stanescu algorithm.

The amount of dissipation $1 - |G(\omega\Delta t)|$and the phase error $|\omega\Delta t - \omega^*\Delta t|/\pi$ are now represented in logarithmic scales in Fig. 1 as a function of $\omega\Delta t$. The RK44 scheme is the most dissipative scheme with for instance at least two orders of magnitude of difference compared to the RK26-Bogey and RK46-NL algorithms for $\omega\Delta t < \pi/2$, i.e. for waves with more than four time steps per period. The amount of dissipation of the RK26-Bogey and RK46-NL schemes is lower than 5×10^{-4} up to $\omega\Delta t = \pi/2$. Dissipation improvement with respect to the RK46-Stanescu algorithm is about one order of magnitude in this range. For higher pulsations, the RK46-Stanescu scheme is unstable and the RK46-NL and RK26-Bogey schemes have similar dissipation properties. The phase errors of the RK46-Stanescu, RK46-NL and RK26-Bogey schemes remain similar for $\omega\Delta t < \pi/2$, they are smaller than 5×10^{-4}. For $\omega\Delta t = \pi/3$ for instance, phase error improvement is about one order of magnitude compared to the RK44 algorithm.

These results are quantitatively illustrated in Table 2 in terms of accuracy limits. Two criteria of accuracy in amplitude and phase defined in [3] are used: $1 - |G\ \ (\omega\Delta t)| < 5\times10^{-4}$ and $\omega^*\Delta t - \omega\Delta t < 5\times10^{-4}$. The RK44 dissipation limit is about ten points per period and phase error limit is about eight points per period. Dissipation limit of the RK46-Stanescu algorithm is about five points per period, and phase error around three points per period. The RK26-Bogey and RK46-NL schemes have dissipation limit of about three points per period and phase error limit close to four points per period. The RK46-NL algorithm is therefore able to resolve accurately at least four-point-per-period waves.

3. Test cases

To illustrate the scheme properties, two test problems are solved: the linear convection of a 1D wave packet and the nonlinear propagation of a 1D Gaussian pressure pulse.

In the first test case [3], the convective wave equation

$$\frac{\partial u}{\partial t} + c\frac{\partial u}{\partial x} = 0, \quad \text{with } c = 1$$

is solved, with a time step derived from the mesh spacing as $\Delta t = \text{CFL}\times\Delta x/c$. The initial disturbance at $t = 0$ is defined as

$$u(x) = \sin\left(\frac{2\pi x}{8\Delta x}\right)\exp\left[-\ln(2)\left(\frac{x}{3\Delta x}\right)^2\right]$$

and plotted in Fig. 2.

Its spectral content is dominated by the wavenumber $k\Delta x = \pi/4$, corresponding to a wave discretized with eight points per wavelength, and has a large bandwidth for $0 \leqslant k\Delta x \leqslant \pi/2$ as shown in [3]. The spatial derivatives are computed with fiftieth-order standard finite differences so that numerical errors due to derivative approximations are negligible compared to time integration errors. Time integration is performed using the classical fourth-order four-stage RK scheme (RK44), the fourth-order six-stage RK developed by Stanescu and Habashi [7] (RK46-Stanescu), the second-order six-stage RK of Bogey and Bailly [3] (RK26-Bogey) and the present algorithm (RK46-NL). The problem is solved for CFL numbers between 0.1 and 1.3 up to $t = 800$, so that

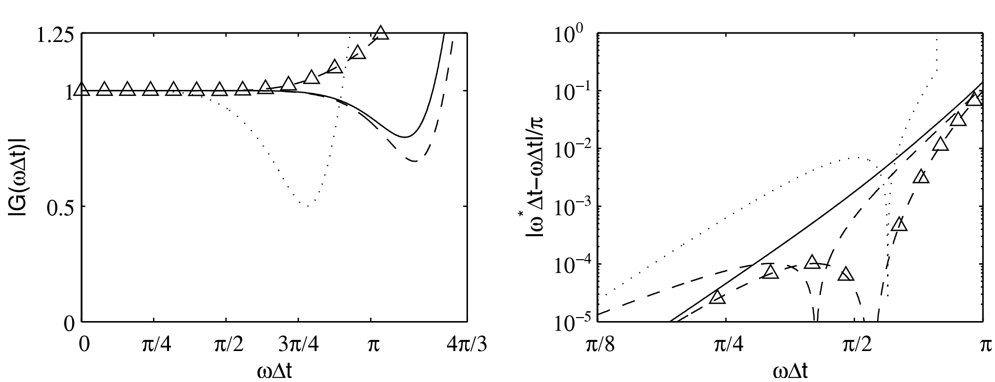

Fig. 1. Left: dissipation, and right: phase error as functions of the angular frequency $\omega\Delta t$ of ······ RK44, standard fourth-order four-stage RK; −Δ−Δ− RK46-Stanescu, fourth-order six-stage RK of Stanescu and Habashi [7]; – – – RK26-Bogey, second-order six-stage RK of Bogey and Bailly [3]; — RK46-NL, present fourth-order six-stage RK.

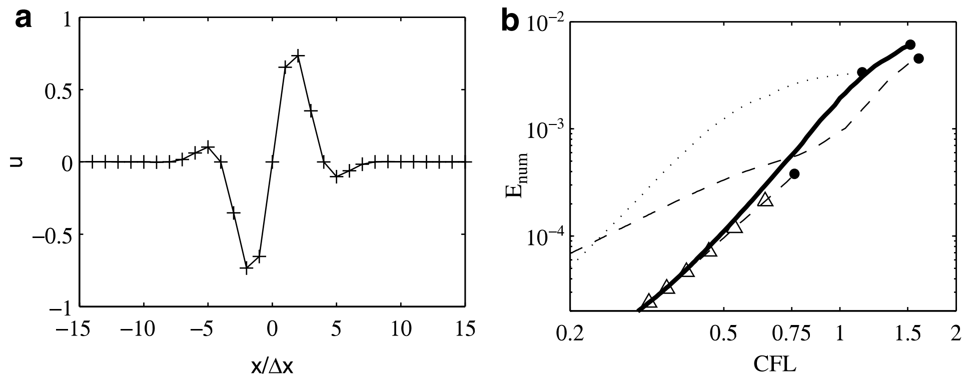

Fig. 2. Linear convection test case: (a) initial perturbation, (b) error as a function of the CFL number using: ⋯⋯ RK44, standard fourth-order four-stage RK; –Δ–Δ– RK46-Stanescu, fourth-order six-stage RK of Stanescu and Habashi [7] ; – – – RK26-Bogey, second-order six-stage RK of Bogey and Bailly [3] ; — RK46-NL, present fourth-order six-stage RK. (●: stability limit for the test case).

the wave is convected over 100 wavelengths. The error rate is evaluated with the L_1-norm as

$$E_{\text{num}} = \frac{1}{N}\sum |u_c - u_e|$$

where u_c and u_e are respectively the computed and the exact vector solution, and $N = 1200$ is the number of mesh points.

The numerical error E_{num} is plotted in Fig. 2 as a function of the CFL number. The stability analysis made in the former Section is confirmed here. The RK46-Stanescu calculation diverges around CFL = 0.75, whereas the RK44 calculation is stable up to CFL = 1.2 and the RK26-Bogey and RK46-NL calculations are stable up to a CFL number of 1.5.

For CFL numbers smaller than 0.6, the error slope is driven by the order of accuracy. The second-order RK26-Bogey algorithm has the smallest slope and thus its error decreases slower than those of the fourth-order algorithms RK44, RK46-Stanescu and RK46-NL as the CFL number is lower. Over the interval $0.2 < \text{CFL} < 0.6$, the RK46-NL and RK46-Stanescu calculations generate a similar error: accuracy improvement is for instance about one order of magnitude compared to the RK44 and RK26-Bogey schemes at CFL = 0.2.

For higher CFL numbers, Taylor series method fails to ensure accuracy since the time step is large and the error is given by the dissipation and dispersion properties of the scheme. The RK44 error is thus larger than those of the RK46-NL and RK26-Bogey algorithms. The RK26-Bogey error becomes smaller than the RK46-NL error as the CFL number increases. Nevertheless they remain of the same order of magnitude.

The second problem is a nonlinear test case. The one-dimensional Euler equations are solved in the dimensionless form:

$$\frac{\partial \mathbf{U}}{\partial t} + \frac{\partial \mathbf{E}}{\partial x} = 0, \quad \text{with } \mathbf{U} = \begin{bmatrix} \rho \\ \rho u \\ \rho e_t \end{bmatrix} \quad \text{and} \quad \mathbf{E} = \begin{bmatrix} \rho \\ \rho u^2 + p \\ u(\rho e_t + p) \end{bmatrix}$$

where ρ is the density, u the velocity, p the pressure and the total energy is given by $e_t = p/(\gamma - 1) + \rho u^2/2$ with $\gamma = 1.4$. The spatial derivatives are computed with thirtieth-order standard finite differences with $\Delta x = 1$. The computational domain contains $N = 800$ points. To highlight the need to use the low-storage formulation of Williamson [6] to ensure fourth-order accuracy when nonlinear operators are involved, the test case has also been solved with the RK46-L algorithm.

The initial perturbation is a Gaussian pressure pulse with high amplitude to induce nonlinear propagation effects:

$$\begin{cases} \rho = 1 \\ u = 0 \\ p = \dfrac{1}{\gamma} + \Delta p \exp(-\alpha x^2) \end{cases}$$

where $\alpha = 0.05$ and $\Delta p = 0.015$. It is propagated up to $t = 300$ for various $\text{CFL} = c\Delta x/\Delta t$ numbers, where the sound speed $c = 1$. The solution computed for CFL = 0.01 is taken as the reference solution. The initial disturbance and the reference solution are plotted in Fig. 3. Wavefront steepening due to nonlinear phenomena is clearly visible on the reference solution at $t = 300$. The error is then computed with the L_1-norm as

$$E_{\text{num}} = \frac{1}{N}\sum |p_c - p_{\text{ref}}|$$

where p_c is the calculated pressure and p_{ref} is the reference solution.

The numerical error E_{num} is plotted in Fig. 4 as a function of the CFL number. As for the linear convection test case, the RK46-Stanescu algorithm is less stable than the other algorithms. It becomes unstable around CFL = 0.8 whereas the other schemes can be used almost up to CFL = 1.3.

For CFL < 0.5, the order of accuracy gives the slope of the error curve. The RK44 error has thus a faster decrease than second-order RK26-Bogey error as the CFL number decreases. As expected, the RK46-L

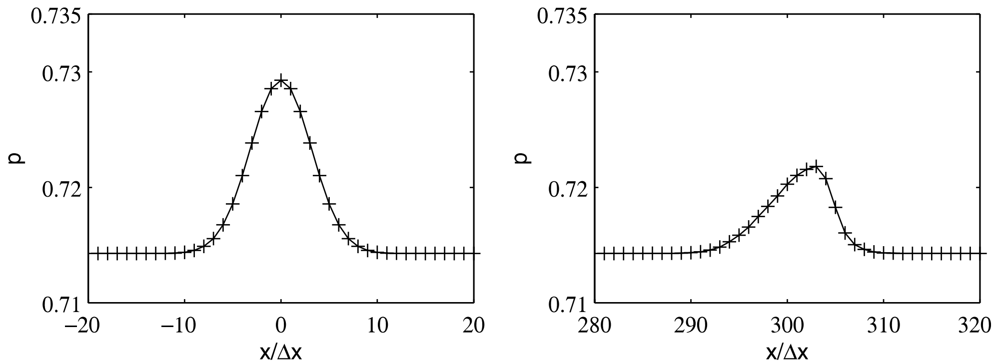

Fig. 3. Left: initial perturbation, and right: reference solution at $t = 300$ for the nonlinear propagation test case.

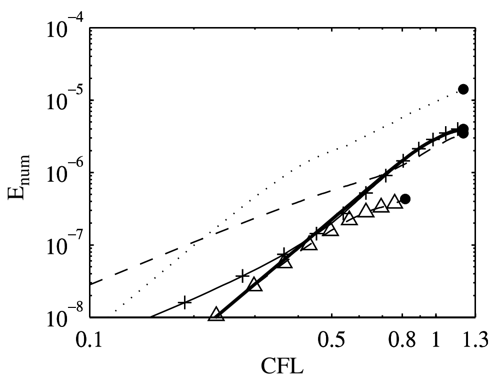

Fig. 4. Nonlinear propagation test case: error as a function of the CFL number using: ⋯⋯ RK44, standard fourth-order four-stage RK; −Δ−Δ− RK46-Stanescu, fourth-order six-stage RK of Stanescu and Habashi [7] ; −−− RK26-Bogey, second-order six-stage RK of Bogey and Bailly [3] ; −+−+− RK46-L, present fourth-order six-stage RK; — RK46-NL, present fourth-order six-stage RK. (●: stability limit for the test case).

scheme is of second order for this test case whereas it is fourth-order for linear operators. The RK46-NL and RK46-Stanescu algorithms are of order four and the more precise algorithms for CFL < 0.5. Difference in precision is about one order of magnitude compared to the RK44 algorithm at CFL = 0.3. For CFL > 0.5, the error is no longer given by the order of accuracy. This part of the error curve is driven by the dissipation and the dispersion of the schemes: the RK46-NL and RK46-L errors are very close to each other as the two algorithms have similar dispersion and dissipation properties. In addition, the RK26-Bogey algorithm becomes slightly more accurate than the RK46-NL scheme.

For this test problem, the error is observed to be driven by the order of accuracy in nonlinear for small CFL numbers and by dissipation and dispersion properties for high CFL numbers. The RK46-NL algorithm is therefore accurate on both intervals thanks to the linear optimization and to its fourth-order accuracy.

4. Conclusion

An explicit low-storage fourth-order six-stage Runge–Kutta scheme, optimized in the Fourier space, has been provided for time integration. The algorithm has a large stability range, it is stable at least for 1.6-point-per-period waves. Numerical accuracy has been investigated through dispersion et dissipation properties: the proposed scheme resolves waves with at least four time steps per period. In addition, an accuracy of order four is achieved for linear and nonlinear operators. Linear and nonlinear propagation test cases have then been solved. It turns out that for low frequencies, precision of the time integration is ensured by the fourth-order accuracy and for high frequencies, the algorithm is still accurate thanks to the linear optimization.

References

[1] Tam CKW, Webb JC. Dispersion-relation-preserving finite difference schemes for computational acoustics. J Comput Phys 1993; 107:262–81.
[2] Lele SK. Compact finite difference schemes with spectral-like resolution. J Comput Phys 1992;103:16–42.
[3] Bogey C, Bailly C. A family of low-dispersive and low-dissipative explicit schemes for flow noise and noise computations. J Comput Phys 2003;194:194–214.
[4] Bogey C, Bailly C, Juvé D. Noise investigation of a high subsonic, moderate Reynolds number jet using a compressible LES. Theoret Comput Fluid Dyn 2003;16:273–97.
[5] Hu FQ, Hussaini MY, Manthey JL. Low-dissipation and low-dispersion Runge–Kutta schemes for computational acoustics. J Comput Phys 1996;124:177–91.
[6] Williamson JH. Low-storage Runge–Kutta schemes. J Comput Phys 1980;35:48–56.
[7] Stanescu D, Habashi WG. 2N-storage low-dissipation and dispersion Runge–Kutta schemes for computational acoustics. J Comput Phys 1998;143:674–81.
[8] Calvo M, Franco JM, Rández L. A new minimum storage Runge–Kutta scheme for computational acoustics. J Comput Phys 2004; 201:1–12.
[9] Berland J, Bogey C, Bailly C. Optimized explicit schemes: matching and boundary schemes, and fourth-order Runge–Kutta algorithm. 10th AIAA/CEAS Aeroacoustic Conference, 10–12 May 2004, Manchester, UK, AIAA Paper 2004–2814.